Multifrequency complementary phase-coded radar signal

N.Levanon

Abstract: A multifrequency radar signal is considered. It uses M subcarriers simultaneously. The subcarriers are phase modulated by M different sequences that constitute a complementary set. Such a set can be constructed, for example, from the M cyclic shifts of a perfect phase-coded sequence of length M (e.g. P4). The subcarriers are separated by the inverse of the duration of a phase element t_b, yielding orthogonal frequency division multiplexing (OFDM), well known in communications. A single pulse of such a signal exhibits a thumbtack ambiguity function with delay resolution of t_b/M. The power spectrum is relatively flat, with width of M/t_b. The signal can be constructed by power combining M fixed-amplitude signals. The resulting signal, however, is of variable amplitude. The peak-to-mean envelope power ratio can be maintained below 2. A train of complementary pulses and a weight function along the frequency axis are useful for further sidelobe reduction.

1 Introduction

Range (delay) resolution is inversely related to the radar signal bandwidth. The quest for higher bandwidth usually follows shorter bit duration in digital phase modulated signals, or wider frequency deviation in analogue frequency modulated signals. In radio communications, where it is advantageous to increase bit-rate without shortening the bit duration, one solution is the use of a modulation technique known as orthogonal frequency division multiplexing (OFDM). The basic idea of OFDM is to replace transmitting serially M short modulation symbols, each of duration t_c, by transmitting M long symbols, each of duration $t_b = Mt_c$, in parallel, on M different subcarriers. In OFDM the subcarriers are separated by $1/t_b$, which ensures that the subcarrier frequencies are orthogonal and phase continuity is maintained from one symbol to the next. OFDM is the suggested technique for digital audio broadcasting [1] and other applications.

Simultaneous use of several subcarriers in radar was recently reported by Jankiraman *et al.* [2]. The PANDORA [2] FMCW radar achieves a bandwidth of 384 MHz, by using 8 linear-FM (LFM) channels, each sweeping 48 MHz. Together with guard bands, the bandwidth totals 776 MHz. A multifrequency signal is characterised by varying amplitude. Amplifying such a signal requires linear power amplifiers (LPA), which are relatively inefficient. Much of Jankiraman's paper is devoted to issues of power combining and amplification.

A modern replacement of the analogue LFM signal is a digital phase-coded signal, in particular, the P3 and P4 signals [3], whose phase sequences are samples from the phase history of a LFM signal. An analogy to the FMCW multifrequency approach would have suggested repeating the same phase-coded modulation sequence on all M subcarriers. We found that lower autocorrelation sidelobs are reached when the M sequences are different from each other and constitute a complementary set. We will call such a signal multifrequency complementary phase coded (MCPC) signal. This paper describes several versions of the MCPC signal and compares its performances to P4, Huffman [4, 5] and Costas [6] signals.

IEE Proceedings online no. 20000734

DOI: 10.1049/ip-rsn:20000734

Paper first received 7th March and in revised form 10th July 2000

The author is with the Department of Electrical Engineering - Systems, Tel-Aviv University, PO Box 39040, Tel Aviv, 69978, Israel

2 MCPC based on all cyclic shifts of P4

2.1 The signal

The phase sequence of a P4 signal is described by

$$\phi_m = \frac{\pi}{M}(m-1)^2 - \pi(m-1), \quad m = 1, 2, \ldots, M \qquad (1)$$

P4 and P3 signals exhibit ideal periodic autocorrelation, namely zero periodic autocorrelation sidelobes. Deducing from simultaneous transmission of LFM pulses would have led us to suggest repeating the same phase sequence on all M subcarriers. However, phase-coded signals yield an additional degree of freedom in the form of cyclic shift. Popovic [7] has shown that all the different cyclic time shifted versions of any sequence having an ideal periodic autocorrelation function, form a complementary set.

A complex valued sequence X_i, whose kth element is $s_i(k)$, forms a complementary set if the sum $Z(p)$ of the aperiodic autocorrelation function R_i of all sequences from the set is equal to zero for all nonzero time shifts p, i.e.

$$Z(p) = \sum_{i=0}^{M-1} \sum_{k=0}^{M-1-p} s_i(k) s_i^*(k+p) = \begin{cases} \sum_{i=0}^{M-1} R_i(0), & p = 0 \\ 0, & p \neq 0 \end{cases} \qquad (2)$$

where * denotes complex conjugate, p is the (positive) time shift, and $R_i(0)$ is the energy of the sequence X_i. When the set

has only two sequences (a complementary pair), the two sequences (of equal length M) must have aperiodic autocorrelation functions whose sidelobes are equal in magnitude but opposite in sign. The sum of the two autocorrelation functions has a peak of $2M$ and a sidelobe level of zero.

In order to take advantage of this autocorrelation property in radar signals [8], the sequences must be separated, e.g. in time (two different pulses). With large time separation, even a small Doppler shift causes a large phase shift, and the sequences quickly lose the property of cancelled autocorrelation sidelobes.

The use of multiple subcarriers provides another possibility of separation: frequency. We will investigate the properties of such a signal using a simple complementary set constituted of the five shifts of a P4 signal of length 5. The basic phase sequence is obtained by using $M=5$ in eqn. 1. It appears in the top row of Table 1. The remaining rows are all the remaining cyclic shifts.

Following the OFDM approach, the $M\ (=5)$ sequences will be transmitted on M subcarriers, separated by $f_s = 1/t_b$, where t_b is the duration of each phase element (bit). The complex envelope of the transmitted signal is therefore

$$u(t) = \begin{cases} \sum_{n=1}^{M} W_n \exp\left\{ j\left[2\pi t f_s \left(\frac{M+1}{2} - n \right) + \theta_n \right] \right\} \\ \qquad \sum_{m=1}^{M} u_{n,m}[t-(m-1)t_b],\ 0 \le t \le Mt_b \\ 0 \quad , \quad \text{elsewhere} \end{cases} \tag{3}$$

where

$$u_{n,m}(t) = \begin{cases} \exp(j\phi_{n,m}) \ , \ 0 \le t \le t_b \\ 0 \quad , \quad \text{elsewhere} \end{cases} \tag{4}$$

$\phi_{n,m}$ is the mth phase element of the nth sequence, θ_n is an arbitrary phase shift added by the transmitter hardware to each carrier (known to the receiver) and W_n is the amplitude weight assigned to the nth subcarrier. eqns. 3 and 4 describe the complex envelope of an $M \times M$ MCPC signal.

2.2 Comparison between $M \times M$ MCPC ($M=5$) and P4 ($N=25$)

Fig. 1 compares schematically a 25 chip P4 pulse (Fig. 1*a*) and a 5×5 MCPC pulse (Fig. 1*b*). The P4 pulse is constructed from N phase modulation chips, each of duration t_c. The typical autocorrelation of a P4 pulse exhibits a narrow main lobe at zero delay, a first null at t_c, and low sidelobes extending as far as the pulse duration Nt_c. The power spectral density of P4 resembles a $\sin^2(\pi f t_c)/(\pi f t_c)^2$ function. The first null is at $f = 1/t_c$ and the spectrum peak sidelobe level is -26 dB.

The schematic description of the MCPC pulse (Fig. 1*b*), shows $M(=5)$ sequences modulating M subcarriers. The bit duration t_b in each sequence was chosen to be M times longer than t_c. This will yield an autocorrelation mainlobe width similar to a P4 pulse with $M^2(=25)$ chips. We will

Table 1: Set of five complementary phase coded sequences

Seq. 1	0°	− 144°	− 216°	− 216°	− 144°
2	− 144°	− 216°	− 216°	− 144°	0°
3	− 216°	− 216°	− 144°	0°	− 144°
4	− 216°	− 144°	0°	− 144°	− 216°
5	− 144°	0°	− 144°	− 216°	− 216°

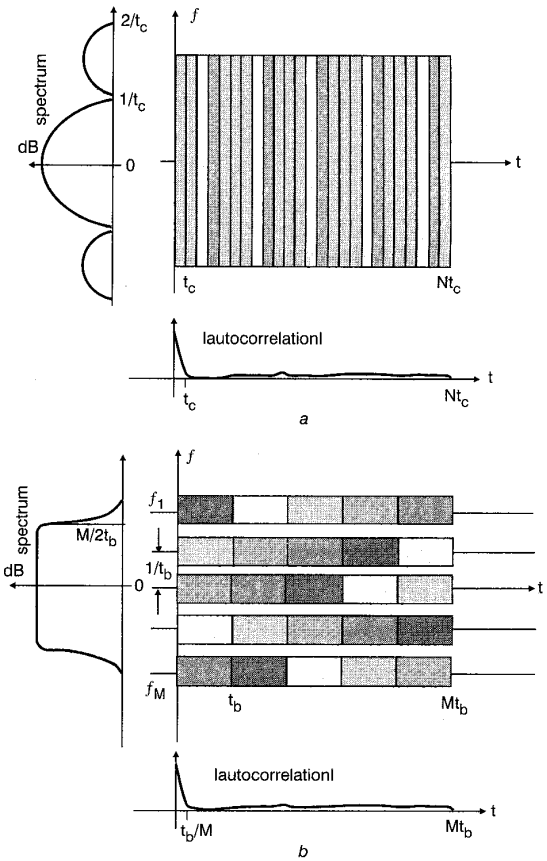

Fig. 1 *Schematic comparison between $M \times M$ MCPC and M^2 element P4*

a P4
b $M \times M$ MCPC

also show that the MCPC pulse exhibits a more efficient spectrum usage. As depicted in Fig. 1, the power spectrum is nearly rectangular with cutoff at $f \approx M/(2t_b)$.

The ambiguity function and its zero-Doppler cut (the magnitude of the autocorrelation) of $u(t)$ depends on the permutation of the five sequences along the five subcarriers $(2f_s, f_s, 0, -f_s, -2f_s)$. A preferred (low sidelobe RMS) permutation results in the autocorrelation (magnitude) shown in Fig. 2*a*. Note that the first null appears at $t_b/5$. This means that, by using five subcarriers, we have created an autocorrelation resembling that of a single-frequency signal that, over the same total duration, has five times as many bits. Note also the nulls of the autocorrelation function at multiples of t_b. These nulls result from the combination of the orthogonality ($f_s = 1/t_b$) and the complementary set. It is interesting to compare the autocorrelation of the MCPC pulse with the autocorrelation of a P4 signal of length 25. Its magnitude is plotted in Fig. 2*b*. The phase sequence of a P4 signal with 25 elements uses 13 distinct phase values. This compares with only three distinct values in Table 1. Two other aspects to compare are the occupied spectrum and the Doppler sensitivity. Fig. 3 displays the corresponding power spectral densities (PSD) of the MCPC and the P4 pulses, obtained from the Fourier transform of their respective autocorrelation functions in Fig. 2. In general, the MCPC signals exhibit a more narrow and flat spectrum (of the complex envelope) extending as far as

$$f_{\max} \approx \frac{M}{2t_b} \tag{5}$$

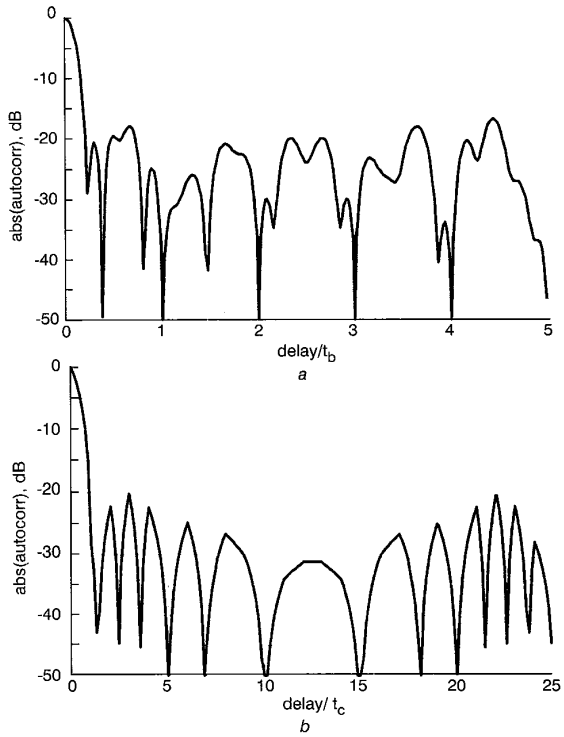

Fig. 2 *Autocorrelation functions of 5 × 5 MCPC and 25-element P4*
Identical horizontal scale (since $t_b = 5t_c$)
a MCPC, sequence order 3 5 2 1 4
b P4

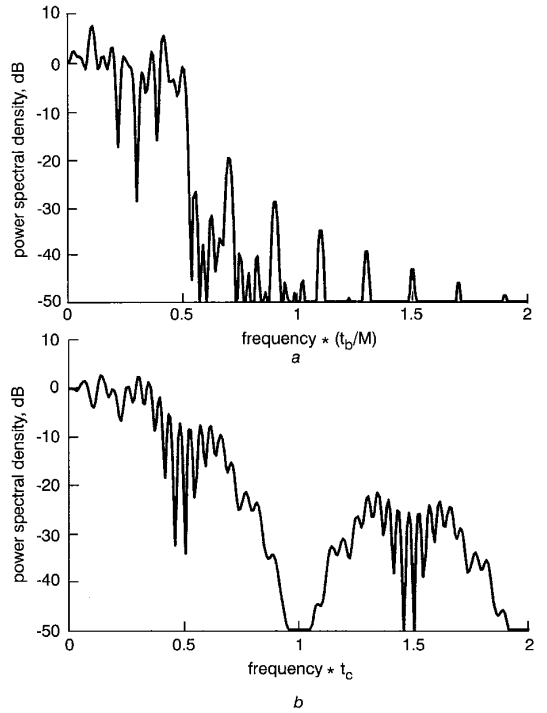

Fig. 3 *Power spectra of 5 × 5 MCPC and 25-element P4*
Identical horizontal scale (since $t_b = 5t_c$)
a MCPC, sequences order 3 5 2 1 4
b P4

The bandwidth of the band-pass signal around its centre frequency will therefore be:

$$\mathrm{BW} = 2f_{\max} \approx \frac{M}{t_b} \tag{6}$$

The sensitivity to Doppler shift is described by the ambiguity function. The 1st and 2nd quadrants are shown in Fig. 4 for the 5 × 5 MCPC pulse, and in Fig. 5 for the 25-element P4 pulse. The ambiguity function of the MCPC pulse does not exhibit the ridge seen in the ambiguity function of the P4 pulse (also typical of LFM). Zooming will reveal that there is no rapid increase of the sidelobe level with small Doppler shift. The Doppler scales in both figures are identical, extending from 0 to 12 times the inverse of the pulse duration. The delay scales are also identical extending over ± the pulse duration.

The performances of the MCPC signal were calculated assuming no hardware inserted phase shifts and no frequency weighting, namely, $\theta_n = 0$, $W_n = 1$, for $n = 1, \ldots, M$ were assumed in eqn. 3. Phase shifts other than zero will slightly modify the spectrum and the sidelobe patterns of the ambiguity function. The resulting effect will be similar to that of using a different order of the sequences. The role of frequency weighting will be discussed in Section 5.

2.3 Comparison between M × M MCPC (M = 9) and P4 (N = 25)

From a spectral-width point of view, it is more reasonable to compare the 25-element P4 signal with a 9 × 9 MCPC

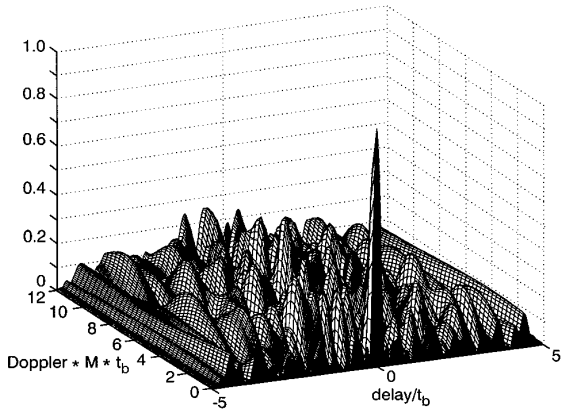

Fig. 4 *Ambiguity function (1st and 2nd quadrants) of 5 × 5 MCPC pulse*
Sequence order 3 5 2 1 4

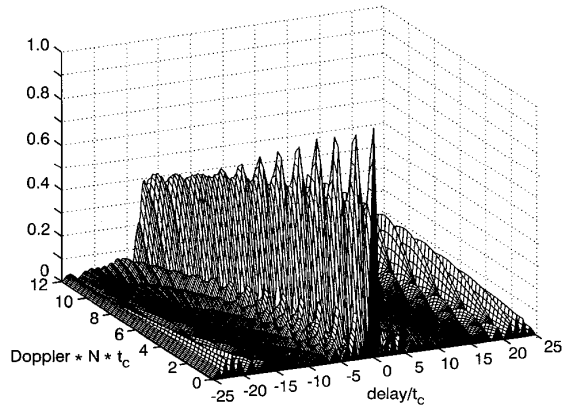

Fig. 5 *Ambiguity function (1st and 2nd quadrants) of 25 element P4 pulse*

signal. The sequence order of the MCPC signal is that order which yields the lowest RMS sidelobe level, found by an exhaustive search (valid as long as $\theta_n = 0$, $n = 1, \ldots, M$). The autocorrelation (in dB) of both signals is given in Fig. 6*a*. It reveals a similar peak-sidelobe level of -20 dB, yet a much narrower mainlobe of the MCPC signal. The ratio of the first delay nulls is

$$\frac{\tau_{\text{null,MCPC}}}{\tau_{\text{null,P4}}} = \frac{N}{M^2} = \frac{25}{81} \simeq 0.3 \tag{7}$$

The power spectral density of both signals is given in Fig. 6*b*. It explains why we consider the 25-element P4 signal to occupy the same spectrum as a 9×9 MCPC signal.

Studying MCPC signals of other sizes reveals a clear sidelobe level drop as M increases. For $M \leq 13$, an empirical relationship of the sidelobe RMS value in dB is $20\log(SL_{\text{RMS}}) \simeq -(1.13M + 17.7)$. The best found permutations were used to obtain the relationship. However, for $M \geq 11$ the large number of permutations ($11! \approx 4 \times 10^7$) excludes an exhaustive search. The large number of permutations could be exploited when many similar radar units must coexist in physical proximity, e.g. in automotive radar applications.

3 Peak-to-mean envelope power ratio (PMEPR)

A major drawback of the MCPC signal is its varying envelope. If the signal generator contains a power amplifier, it becomes desirable to reduce the peak-to-mean envelope power ratio (PMEPR) as much as possible. The orthogonality of the MCPC signal implies that, over a bit duration, one subcarrier has no effect on the others. Hence, if each subcarrier is of unit power then the mean power of the M subcarriers must be M. The instantaneous peak power during a bit can be at most M^2. We can therefore conclude that, in general

$$\text{PMEPR} \leq M \tag{8}$$

However, we found out, numerically, that when the MCPC is based on all the cyclic shifts of a P4 signal, and $M \geq 4$, and the sequence order is also a cyclic shift, namely

$$\{k, k+1, \ldots, M-1, M, 1, 2, \ldots, k-1\}$$
$$\text{or } \{k, k-1, \ldots, 2, 1, M, M-1, \ldots, k+1\} \tag{9}$$

then

$$\text{PMEPR} \leq 2.015 \tag{10}$$

Note that Boyd [9] has pointed out the result in eqn. 10 for the case of a multitone symbol in which the phase sequence (along the M frequencies) follows a P3 phase sequence. (Boyd calls it 'Newman phases'.)

The lower PMEPR when the order of sequences is as in eqn. 9 is demonstrated in Figs. 7*a* and *b*, where the real envelopes of 5×5 MCPC signals based on P4 are given

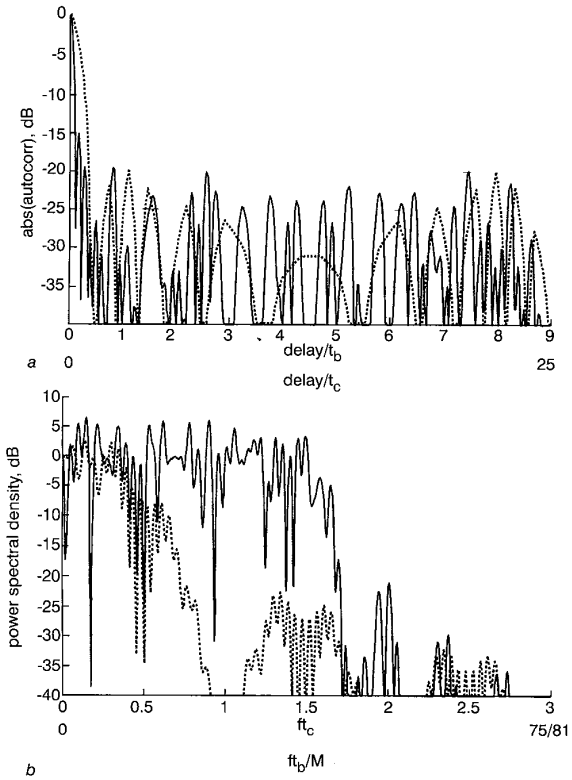

Fig. 6 *Autocorrelation functions and power spectra of 9×9 MCPC and a 25-element P4*

—— MCPC (5 3 1 8 6 4 2 9 7)
---- P4
a Autocorrelation functions
b Power spectra

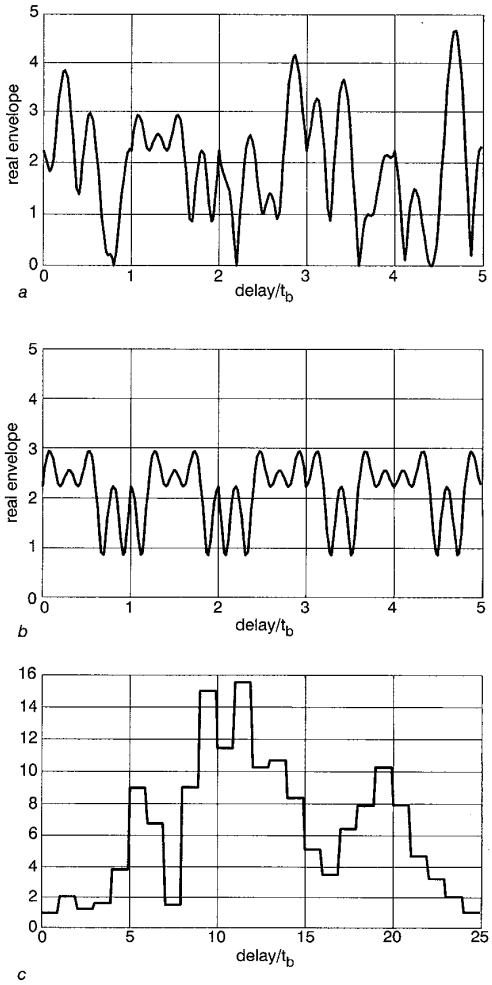

Fig. 7 *Real envelopes of two permutations of 5×5 MCPC pulse and Huffman pulse*

PMEPR = peak to mean envelope power ratio
a MCPC 3 5 2 1 4, PMEPR = 4.37
b MCPC 3 4 5 1 2, PMEPR = 1.73
c Huffman, seed = 456, PMEPR = 4.12

for the sequence orders {35214} and {34512}, respectively. The latter one meets the criteria in eqn. 9. The corresponding PMEPRs are 4.37 and 1.73. For comparison, Fig. 7*c* presents the real envelope of a 25 element Huffman signal, which is also of variable envelope, and which will be discussed in Section 7.

4 Train of complementary MCPC pulses

A train of M MCPC pulses can be complementary in time as well as in frequency. This happens when each pulse in the train exhibits a different order of sequences such that a set of complementary phase sequences is obtained in each frequency. The autocorrelation sidelobes are further reduced as demonstrated by comparing Fig. 8*a* to Fig. 2*a*. Both pertain to a 5×5 MCPC signal. The order of sequences in the five pulses is outlined within the drawing. We note from Fig. 8*a* that the sidelobe reduction applies to all but the sidelobes within the first bit. This should be expected because a complementary set yields zero autocorrelation sidelobes only for $|\tau| > t_b$.

The delay axis in Fig. 8 is limited to the duration of a pulse ($= Mt_b$). The autocorrelation within that delay is not affected by the pulse interval T as long as T is larger then twice the pulse width, namely $T > 2Mt_b$. The pulse interval does affect the ambiguity function for nonzero Doppler.

The dramatic improvement in sidelobe reduction for $t_b < |\tau| < Mt_b$ by a train of complementary MCPC pulses invites a method for further sidelobe reduction in the delay range of $|\tau| < t_b$. In the next Section we will demonstrate how this is achieved by applying weights along the frequency axis.

We will postpone presenting an ambiguity functions of a complementary train of MCPC pulses until after the discussion on weighting, in order to demonstrate the combined effect.

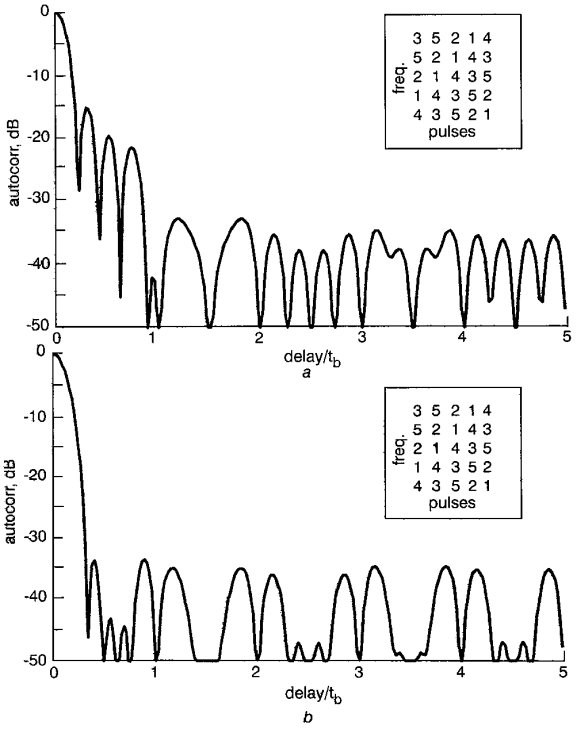

Fig. 8 *Autocorrelation functions of train of five 5 × 5 MCPC pulses*
The delay scale extends for the duration of one pulse only
a Without frequency weighting
b With frequency weighting, weight power = 0.38

5 Frequency weighting of a train of complementary MCPC pulses

Frequency weighting is a well-established method for reducing autocorrelation sidelobes in linear FM radar signals [8]. We found out that it was not very effective in a single MCPC pulse because it yielded meaningful sidelobe reduction only over the limited delay range $|\tau| < t_b$, but did not help over the larger remaining delay range of $t_b < |\tau| < Mt_b$. However, once we found out that a complementary train of MCPC pulses dramatically reduces sidelobes in that larger delay range $t_b < |\tau| < Mt_b$, it became obvious that combining complementary pulse train and frequency weighting can reduce autocorrelation sidelobes over the entire delay range $0 < |\tau| < Mt_b$.

In conventional constant-amplitude radar signals, weighting is usually implemented only at the receiver, in order not to loose the constant-amplitude property of the transmitted signal. This is effectively a deviation from matched filter processing and results in a small SNR loss. In our case, the signal is already of variable amplitude (but of fixed amplitude at each subcarrier). Hence applying different amplitude to each subcarrier adds no difficulty.

Despite the extensive knowledge regarding weighting windows, we limited our numerical trials to a simple family of weighting described by

$$W_n = \left[a_0 + a_1 \cos\frac{2\pi\left(n-\frac{1}{2}\right)}{M}\right]^{\alpha} \quad , \quad n = 1, \ldots M \qquad (11)$$

Note that setting $a_0 = 0.53836$, $a_1 = 0.46164$ and $\alpha = 0.5$ is equivalent to adding a Hamming window at the receiver side. We found out that values of α slightly different from 0.5 yielded smaller peak sidelobes. The weight W_n now multiplies the signal of the nth subcarrier as noted in eqn. 3. To the $M = 5$ MCPC complementary pulse train used in Fig. 8*a*, we added weighting according to eqn. 11. The resulting magnitude of the autocorrelation function is plotted in Fig. 8*b*.

The ambiguity function of a complementary train of M MCPC pulses, with or without weighting, depends on the pulse interval T. The partial ambiguity function plotted in Fig. 9 was obtained for an arbitrary case in which the pulse interval was four times the MCPC pulse duration, namely

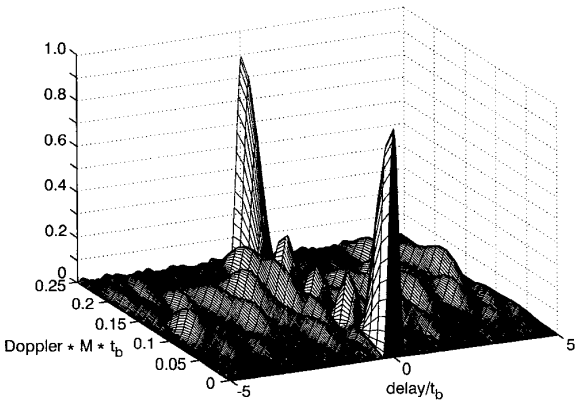

Fig. 9 *Ambiguity function of train of five 5 × 5 MCPC pulses with frequency weighting*
The delay scale extends for the duration of ± one pulse only
Sequence order 3 5 2 1 4; weight power = 0.38

$T = 4Mt_b$ and the weighting was according to eqn. 11. Because of the periodicity in time, the response in Doppler exhibits peaks at multiples of $v = 1/T = 0.25/Mt_b$, the first of which is seen in Fig. 9.

6 MCPC based on two-valued complementary set

The P4 phase sequence used so far to construct the MCPC complementary set is a polyphase code. There are two-valued phase sequences that also exhibit perfect periodic autocorrelation, and can serve to construct a complementary set. One such alternative is the sequences described by Golomb [10]. One example of such a sequence is based on Barker code of length 7 [+ + + − − + −], in which the two phase values are not 0 and 180° but 0 and 138.59°(= arccos(−3/4)). Codes of this type exist for lengths 3, 7, 11, 15, 19, 23, 31, 35, 43, 47, 59, ... For a 23 × 23 MCPC single pulse, based on all the cyclic shifts of the corresponding two-valued perfect sequence, the autocorrelation (magnitude) and the ambiguity function are presented in Figs. 10*a* and 11, respectively. The RMS sidelobe value of the two-valued signal is usually 15% higher than for a polyphase signal of the same size. Adding frequency weight to the above signal alters the sidelobes, mostly within the first bit, as demonstrated in Fig. 12, which zooms on the first two bits.

It is also interesting to compare the autocorrelation of the two-valued signal with one in which the phase values were changed to 0 and 180° (not a complementary set any more, but easier to implement). Degradation in RMS value by about 25% (relative to the ideal two-valued code) is typical. As already pointed out, in all MCPC signals based on complementary sets the autocorrelation is identically zero at multiples of t_b. This property is lost in a non-complementary set, and is one reason for the higher sidelobe RMS value.

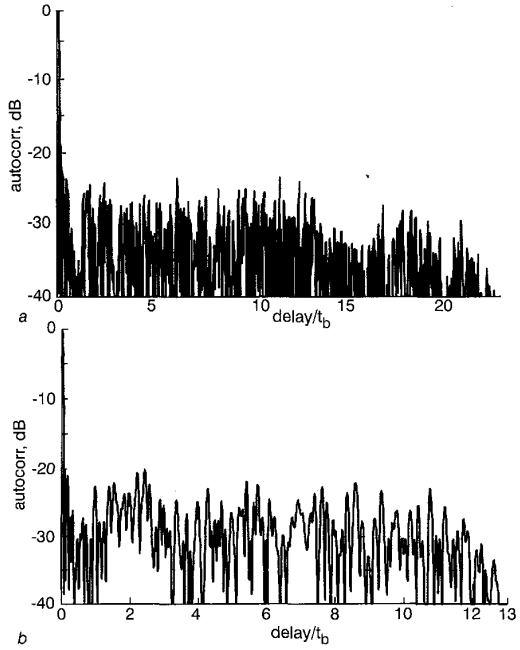

Fig. 10 *Autocorrelation functions of 23 × 23 MCPC pulse based on Golomb's 2-valued sequence and 13 × 13 MCPC pulse based on Ipatov's binary sequence*

a Golomb, weight power = 0
Sequence order 9 5 3 16 23 7 8 21 6 14 15 1 4 17 20 22 10 13 2 8 19 11 12
b Ipatov, weight power = 0.12
Sequence order 5 12 3 1 10 8 11 4 9 13 7 2 6

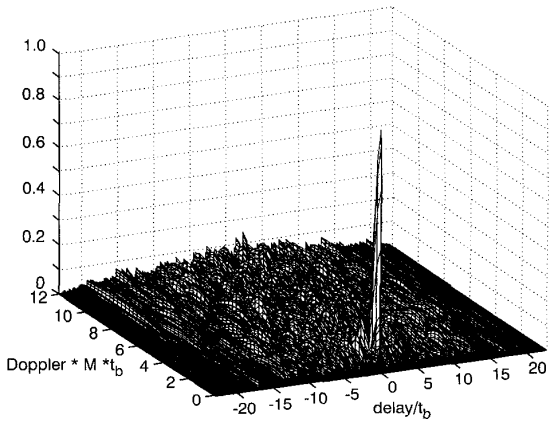

Fig. 11 *Ambiguity function of 23 × 23 MCPC pulse based on Golomb's 2-valued sequence*

0 and 156.443°
Sequence order 9 5 3 16 23 7 8 21 6 14 15 1 4 17 20 22 10 13 2 8 19 11 12

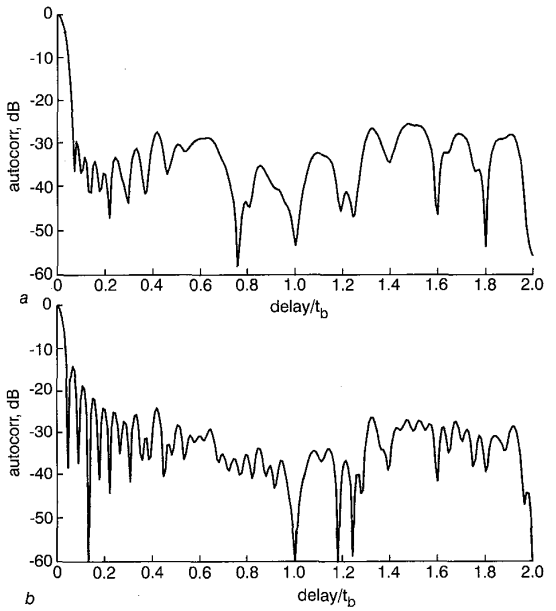

Fig. 12 *Partial autocorrelation function ($0 \le \tau \le 2t_b$) of 23 × 23 MCPC pulse*

0 and 156.443°
Sequence order 9 5 3 16 23 7 18 21 6 14 15 1 4 17 20 22 10 13 2 8 19 11 12
a With frequency weighting, weight power = 0.33
b Without frequency weighting

Implementing two-valued sequences is especially simple if the two are binary values (−1, +1). There are only few square or nearly-square binary complementary sets. Some examples are listed in Table 2 [11].

It is interesting to note the dramatically different ambiguity function of a train of four complementary MCPC pulses based on the 4 × 4 complementary sets (*b*) and (*c*) in Table 2. The ambiguity function in Fig. 13*a*, which corresponds to a frequency-weighted pulse-train based on set (*b*), exhibits perfect zero sidelobes for all but the first bit, for zero Doppler. However, the sidelobes build up rapidly with Doppler. The ambiguity function in Fig. 13*b*, which corresponds to a pulse train based on set (*c*), exhibits low (but not zero) sidelobes for all delays and

Table 2: Complementary binary sets

(a)	(b)	(c)	(d)
+ + +	+ + + +	+ + − +	+ − − − −
− + +	+ − + −	+ − + +	− + + − +
+ − +	+ + − −	− + + +	+ − − − +
+ + −	+ − − +	+ + + −	− − − + −

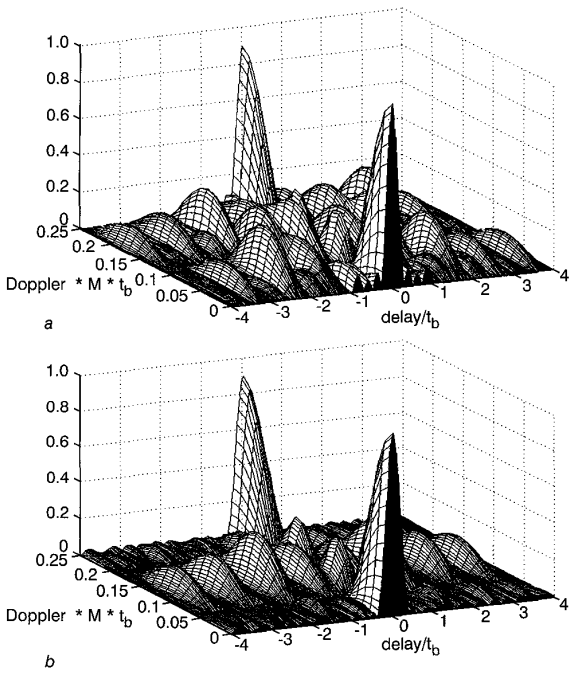

Fig. 13 *Ambiguity functions of train of four 4 × 4 MCPC binary pulses*
a According to Table 2*b*, weight power = 0.13, sequence order 1 4 3 2
b According to Table 2*c*, weight power = 0.33, sequence order 4 1 3 2

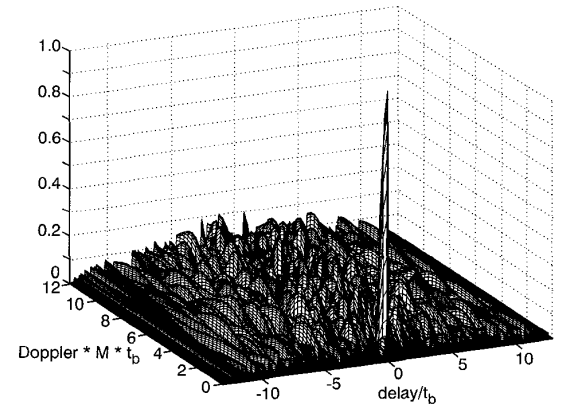

Fig. 14 *Ambiguity function of 13 × 13 MCPC pulse based on Ipatov's binary sequence*
Weight power = 0.12
Sequence order 5 12 3 1 10 8 11 4 9 13 7 2 6

for relatively wide Doppler width. Note that set (*c*) was constructed from all the cyclic shifts of a Barker code of length 4, which has an ideal periodic autocorrelation while set (*b*) is a Hadamard matrix.

There is still another type of MCPC signal that would allow transmitting binary values $(-1, +1)$. It requires, however, a slightly mismatched receiver. This type of MCPC signals is based on the sequences suggested by Ipatov [12]. They yield perfect periodic cross-correlation with a slightly mismatched reference sequence. An example is the length 13 transmitted sequence [1 1 1 1 1 −1 −1 1 1 −1 1 −1 1] which yields perfect periodic cross-correlation with the reference sequence [1 1 1 1 1 −1.5 −1.5 1 1 −1.5 1 −1.5 1].

A frequency weighted 13 × 13 MCPC signal based on all the cyclic shift of the Ipatov signal outlined above, and ordered in one of 13! possible permutations, yielded the cross-correlation (magnitude) and delay-Doppler response presented in Figs. 10*b* and 14, respectively.

7 Comparison with Huffman coded signals

The variable amplitude of the MCPC signal invites comparison with Huffman-coded signals [4, 5]. Huffman signals are constructed from N elements of width t_c, each one modulated in amplitude as well as in phase. The result is nearly ideal autocorrelation (zero sidelobes, except for two small peaks at the edges), which implies nearly perfect $\sin^2(\pi f t_c)/(\pi f t_c)^2$ power spectrum. The length N of the code determines the phase of the elements. The amplitude sequence is determined by the two sidelobe peaks, and by the zero pattern of the z transform of the Huffman sequence. For a given sidelobe peak level there are 2^{N-1} different combinations. The zero pattern combination does not affect the autocorrelation (hence zero-Doppler cut of the ambiguity function), but does affect the ambiguity function at Doppler shifts other than zero and also the real envelope of the signal.

The same mainlobe width as an $M \times M$ MCPC signal will be obtained from an $N = M^2$ element Huffman code. Examples of the real envelope and ambiguity function of a 25-element Huffman signal are given in Figs. 7*c* and 15, respectively. By definition, Huffman signals can be designed with much lower autocorrelation sidelobes than MCPC, but because of their perfect $\sin^2(\pi f t_c)/(\pi f t_c)^2$ power spectrum shape, their spectrum use is less efficient. But the major difference between Huffman and MCPC signals is with regard to implementation. A Huffman signal has to be

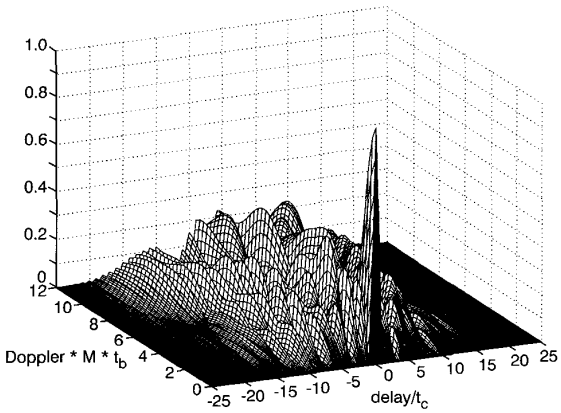

Fig. 15 *Ambiguity function of 25-element Huffman pulse*

generated as one entity and then amplified using linear amplifiers. On the other hand, an MCPC signal can be generated by passive power combination of M different signals, each one of constant amplitude.

8 Comparison with Costas frequency coding

Costas signals [6] achieve pulse compression by intrapulse frequency hopping. During any one of M code elements of duration t_b, only one of M frequencies is used, with no repetitions. The frequencies are separated by $1/t_b$. A Costas signal is the only other coded signal that achieves nearly rectangular spectrum, as does the MCPC signal, and Costas signals achieve that spectral efficiency while maintaining constant envelope. The first autocorrelation null of Costas signal is at t_b/M, like in MCPC. The autocorrelation sidelobe RMS level in Costas signals is generally higher than in equally long MCPC. One example of the ambiguity function of a 5-element Costas signal is given in Fig. 16.

Another way to compare between Costas signals and MCPC is to note that in order to transmit energy of $E = PMt_b$, a Costas signal requires a transmitter of power P, hoping over M frequencies, and using each frequency only for the duration of one t_b. On the other hand, an MCPC signal uses all the frequencies, all the time, by power combining M fixed-amplitude signals each with power P/M.

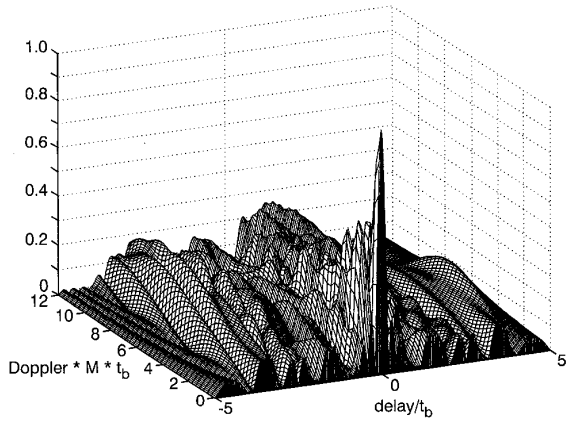

Fig. 16 *Ambiguity function of 5-element Costas pulse*
Sequence order 3 5 2 1 4

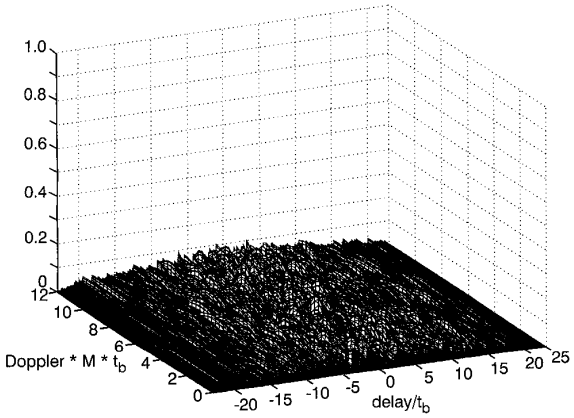

Fig. 17 *Cross-ambiguity function between two different permutations of a 23 × 23 MCPC pulse (based on Golomb's 2-valued sequences)*

It is interesting to note that in the 5×5 MCPC signal described in Table 1, in the permutation with lowest sidelobes [3 5 2 1 4], isolating the 0° phase elements creates a Costas signal.

9 Cross-ambiguity function between two different M × M MCPC signals

For any $M \times M$ MCPC signal there are $M!$ different permutations of ordering the M sequences along the M subcarriers. The many permutations could allow nearly interference-free operation of several MCPC radar instruments in physical proximity. This could be useful in automotive radar applications. When a receiver is matched to one $M \times M$ MCPC signal, and a different $M \times M$ MCPC signal is received with delay and frequency offset (due to different oscillator frequency or Doppler), the output of the receiver as function of time-shift and frequency-shift is called the cross-ambiguity function. The desired property of cross-ambiguity is low peaks everywhere. Fig. 17 presents an example of the cross-ambiguity function between the 23×23 MCPC signals (based on Golomb's 2-value signal used in Fig. 11) and another permutation of it, selected randomly. Note that no coincidence (the same number at the same location) between the two orders guarantees a null at the origin of the cross-ambiguity function.

10 Conclusions

The MCPC signal is a new multifrequency radar signal with several advantages over known radar signals. As P3 and P4 signals, MCPC is a digitally phase modulated signal, but unlike P3 and P4 signals, MCPC exhibits a thumbtack ambiguity function and requires fewer phase values. Like Costas signal, it utilises many subcarriers, but unlike Costas it utilizes all the frequencies all the time. MCPC main drawback is its variable real envelope. However, the MCPC signal can be generated by power combining several fixed-envelope signals. This implementation option is not available for a Huffman coded signal, which is another signal with variable real envelope.

While MCPC is essentially a pulse signal, it inherits its favourable a-periodic autocorrelation from the periodic autocorrelation of the signal it is based on. Hence, the wealth of knowledge on signals with perfect periodic autocorrelation can be utilised for an aperiodic signal. Among signals with perfect periodic autocorrelation, we can find long two-valued phase coded signals, and mismatched binary signals, which are easier to implement than polyphase signals.

Being a multifrequency signal, MCPC yields easily to frequency weighting — useful for autocorrelation sidelobe reduction. Further sidelobes reduction can be reached by using a train of MCPC pulses, if designed to be complementary both along each pulse and along each frequency.

Finally, an $M \times M$ MCPC signal has $M!$ different permutations. The cross-ambiguity between any pair exhibits relatively low peaks, which suggests low mutual interference between nearby radar instruments.

11 References

1 LE FLOCH, B., HALBERT-LASSALLE, R., and CASTELAIN, D.: 'Digital sound broadcasting to mobile receivers', *IEEE Trans. Consum. Electron.*, 1989, **35**, (3), pp. 493–503

2 JANKIRAMAN, M., WESSELS, B.J., and VAN GENDEREN, P.: 'System design and verification of the PANDORA multifrequency radar'. Proceedings of international conference on *Radar Systems*, Brest, France, 17–21 May 1999, Session 1.9
3 KRETSCHMER, F.F., and LEWIS, B.L.: 'Doppler properties of polyphase coded pulse compression waveforms', *IEEE Trans. Aerosp. Electron. Syst.*, 1983, **AES-19**, (4), pp. 521–531
4 HUFFMAN, D.A.: 'The generation of impulse-equivalent pulse trains', *IRE Trans. Inf. Theory*, 1962, **8**, pp. S10–S16
5 ACKROYD, M.H.: 'The design of Huffman sequences', *IEEE Trans. Aerosp. Electron. Syst.*, 1970, **AES-6**, (6), pp. 790–796
6 COSTAS, J.P.: 'A study of a class of detection waveforms having nearly ideal range–Doppler ambiguity function properties', *Proc. IEEE*, 1984, **72**, (8), pp. 996–1009
7 POPOVIC, B.M.: 'Complementary sets based on sequences with ideal periodic autocorrelation', *Electron. Lett.*, 1990, **26**, (18), pp. 1428–1430
8 FARNET, E.C., and STEVENS. G.H.: 'Pulse compression radar,' *in* SKOLNIK, M. (Ed.): 'Radar Handbook' (McGraw-Hill, 1990, 2nd edn.) Ch. 10
9 BOYD, S.: 'Multitone signals with low crest factor', *IEEE Trans. Circuits Syst.*, 1986, **CAS–33**, (10), pp. 1018–1022
10 GOLOMB, S.W.: 'Two-valued sequences with perfect periodic autocorrelation', *IEEE Trans. Aerosp. Electron. Syst.*, 1992, **28**, (2), pp. 383–386
11 TSENG, C.C., and LIU, C.L.: 'Complementary sets of sequences', *IEEE Trans. Inf. Theory*, 1972, **IT–18**, (5), pp. 644–652
12 IPATOV, V.P., and FEDOROV, B.V.: 'Regular binary sequences with small losses in suppressing sidelobes', *Radioelectron. Commun. Syst.*, 1984, **27**, pp. 29–33